nature chemistry

ARTICLES

PUBLISHED ONLINE: 11 NOVEMBER 2012 | DOI: 10.1038/NCHEM.1488

Submolecular control, spectroscopy and imaging of bond-selective chemistry in single functionalized molecules

Ying Jiang[1,2], Qing Huan[1,3], Laura Fabris[4], Guillermo C. Bazan[4] and Wilson Ho[1,5]*

One of the key challenges in chemistry is to break and form bonds selectively in complex organic molecules that possess a range of different functional groups. To do this at the single-molecule level not only provides an opportunity to create custom nanoscale devices, but offers opportunities for the in-depth study of how the molecular electronic structure changes in individual reactions. Here we use a scanning tunnelling microscope (STM) to induce a sequence of targeted bond dissociation and formation steps in single thiol-based π-conjugated molecules adsorbed on a NiAl(110) surface. Furthermore, the electronic resonances of the resulting species were measured by spatially resolved electronic spectroscopy at each reaction step. Specifically, the STM was used to cleave individual acetyl groups and to form Au–S bonds by manipulating single Au atoms. A detailed understanding of the Au–S bond and its non-local influence is fundamentally important for determining the electron transport in thiol-based molecular junction.

Chemical reactions involve the dissociation, rearrangement and formation of individual bonds. An overriding aim of much of chemistry is to break and form specific bonds selectively, namely bond-selective chemistry[1,2]. The scanning tunnelling microscope (STM) has proved to be an ideal tool to induce and view bond-selective chemistry at the single-molecule level, because of the atomic-scale localization and tunability of the energy of the tunnelling electrons[3,4]. Most of the studies on bond-selective chemistry to date addressed small molecules[5–15]. However, the feasibility of initiating a bond-specific reaction within a complex molecule with functional groups is more relevant to molecular nanotechnology, in areas such as molecular electronics, organic solar cells and nanomachines. Furthermore, there are very limited experimental studies on changes in the molecular electronic structure associated with bond dissociation and formation, which provide crucial evidence for orbital hybridization in chemical transformations[16].

Molecules functionalized with thiols are adopted widely for the study of molecular electron transport[17]. However, the measured conductance of thiol-based molecular junctions is distributed over a wide range of values and poorly reproduced by theory[18]. The main reason is the lack of experimental insight into the microscopic geometry of the Au–S bond and the corresponding electronic structure of molecular junctions[19,20]. Therefore, to control the geometry of the Au–S bond at the single-bond level and to probe simultaneously the electronic structure of the molecular junction is of fundamental importance in the field of molecular electronics[21].

Here, we demonstrate the ability to induce a sequence of target-selective bond dissociation and formation steps in a relatively large thiol-based π-conjugated molecule adsorbed on a NiAl(110) surface. Combining the spatial resolution of the STM and the energy tunability of tunnelling electrons for resonant electronic excitation[22–26], at each reaction step we were able to abstract different functional groups selectively from the molecule and monitor the evolution of the molecular electronic structure by spatially resolved electronic spectroscopy. The bond-selective dissociations exposed the sulfur functional groups to activate the formation of the Au–S bonds by manipulating and attaching the single gold atoms to the sulfur atoms at the two ends of the molecule. The details of Au–S bond formation and its influence on the electronic structure of the molecule were determined by the STM. These results underlie the understanding of electron transport in thiol-based molecular junctions[19,21].

Results and discussion

Molecular structure. We carried out the bond-selective chemistry in 1,4-bis(4′-(acetylthio)styryl)benzene (DSB-2S-2Ac) adsorbed on a NiAl(110) surface at 12 K. Originally, DSB-2S-2Ac was designed to contain a π-delocalized electronic structure across the distyrylbenzene (DSB) framework and functional groups (sulfur and acetyl) specific for covalent bond formation to metal surfaces, such as gold[27]. The NiAl(110) surface has pseudogaps in the projected bulk band structure in parts of the Brillouin zone, which lead to the depletion of the local density of states (DOS) between 1.0 and 2.5 eV above the Fermi level[28]. Therefore, the hybridization between the molecular resonances and substrate states is reduced significantly in the energy-gap region, which makes it possible to monitor the molecular resonances at each step of the reaction by measuring the energetic shifts and imaging their spatial distributions.

Figure 1a shows schematic models for two rotational isomers of DSB-2S-2Ac (**I** and **II**, respectively), which can be distinguished by their different symmetries. DSB-2S-2Ac can either be centrosymmetric (**I**) or have a mirror plane that bisects the central aromatic ring (**II**). As shown in the high-resolution STM topographic images (Fig. 1b,c), DSB-2S-2Ac (**I**) exhibits a 'kink' in the middle, but DSB-2S-2Ac (**II**) has a 'belly' instead. These features arise from the π-orbitals of the DSB framework[27]. The enhanced apparent heights at the ends of the molecules suggest that DSB-2S-2Ac adsorbs on the NiAl(110) surface through the lone pair of electrons

[1]Department of Physics and Astronomy, University of California, Irvine, California 92697-4575, USA, [2]International Center for Quantum Materials, Peking University, Beijing, China 100871, [3]Institute of Physics, Chinese Academy of Sciences, Beijing, China 100190, [4]Department of Materials Engineering and Chemistry & Biochemistry, University of California, Santa Barbara, California 93106-9510, USA, [5]Department of Chemistry, University of California, Irvine, California 92697-4575, USA. *e-mail: wilsonho@uci.edu

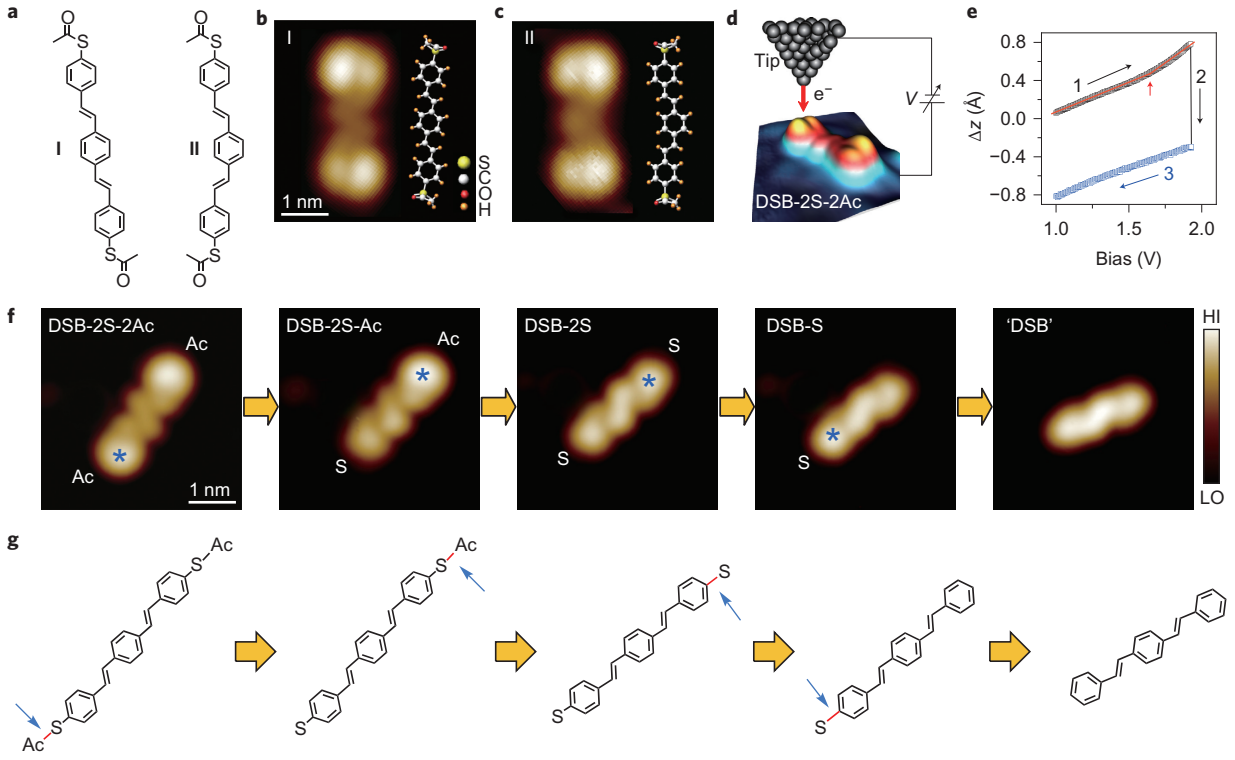

Figure 1 | Stepwise dissociation sequence of the DSB-2S-2Ac molecule. a, Schematic models for two rotational isomers of DSB-2S-2Ac molecules, noted as **I** and **II**. **b**,**c**, STM topographies of the DSB-2S-2Ac (**I**) and (**II**), respectively. Set point: $V = 2.2$ V and $I = 50$ pA. Inserts: ball-and-stick models for the two isomers, scaled (×1.5) to the size of the molecules for comparison. **d**, Schematic drawing of the selective dissociation of different functional groups by injecting electrons at precise locations in the molecule. **e**, The typical Δz–V characteristics in the dissociation event of a DSB-2S-2Ac molecule. The red arrow indicates the bias at which the slope of the curve starts to increase because of the emergence of Ac-derived states. Step 1, the sample bias is ramped up from 1 V at a constant current of 1 nA; step 2, the tip height encounters a sudden jump on dissociation of the acetyl group; step 3, the bias is immediately ramped down to 1 V. **f**,**g**, Topographies and corresponding schematics, scaled (×2.3) for clarity, of the different products in the dissociation sequence. Set point: $V = 1.6$ V and $I = 50$ pA. The asterisks in (**f**) indicate the locations at which the electrons were injected with the STM tip. The small arrows (blue) in (**g**) denote the bonds to be broken in the different steps for the dissociation sequence. HI = high, LO = low.

on the sulfur atom, with the S–Ac bond pointing partially away from the surface (see the ball-and-stick models in Fig. 1b,c). Interestingly, the terminal protrusion of the molecule consists of two distinct lobes with one larger than the other. When the schematic models of DSB-2S-2Ac are superimposed onto the corresponding STM topographies, the two lobes coincide neatly with the oxygen atom and the methyl in the acetyl group. The larger lobes (or smaller ones) always point in the opposite direction in DSB-2S-2Ac (**I**) or to the same side in DSB-2S-2Ac (**II**) so that the symmetries of the DSB molecules are preserved.

Single-bond dissociation sequence. The functional groups in DSB-2S-2Ac can be abstracted one after the other by injecting electrons of different energies from the STM tip at precise locations for bond-breaking within the molecule (Fig. 1d). To achieve the controlled bond rupture and determine precisely the threshold bias for the dissociation, we slowly ramped up the sample bias under the constant current mode (for details see Fig. 1e and Methods). In this manner we were able to strip off two acetyl groups and two sulfur atoms in a stepwise fashion from DSB-2S-2Ac (**I**), as shown in Fig. 1f. Although the acetyl groups always disappear after the dissociation, occasionally the abstracted sulfur atoms can be trapped on the surface (Supplementary Fig. S1). Schematic drawings that summarize the dissociation sequence are shown in Fig. 1g, in which the specific bonds to be broken are indicated by the blue arrows. By analysing different dissociation events in over 50 molecules, the threshold biases for abstracting the acetyl groups and the sulfur atoms were determined as 1.80 ± 0.20 V and 2.30 ± 0.15 V, respectively. These voltages are lower than the threshold voltage for breaking C–H and C–C bonds. It is not until raising the bias above 3.0 V that dehydrogenation or even decomposition can occur (Supplementary Fig. S2), in agreement with the dissociation of benzene and pyridine molecules adsorbed on Cu(100) (ref. 29).

The influence of the different functional groups on the electronic structure of the molecule can be revealed by studying the energetic shifts and the spatial distributions of the molecular resonances at each reaction step. Figure 2 displays the dI/dV images (middle column) and spatially resolved dI/dV spectra (right column) of the molecules terminated with different functional groups. The dI/dV spectra were taken at four key locations on the molecule, indicated as 1, 2, 3 and 4 in the dI/dV images.

The dI/dV spectrum of the intact DSB-2S-2Ac molecule shows a broad peak, which can be deconvoluted into two Gaussian peaks centred around 1.58 V and 1.73 V (right column, Fig. 2a). The intensity of the 1.73 V peak increases significantly from the middle (1 and 2) to the ends (3 and 4) of the molecule. The dI/dV image obtained at the 1.58 V peak exhibits a delocalized orbital that spans the entire molecule (middle column, Fig. 2a). In contrast, the state at 1.73 V is relatively localized in four disconnected lobes at the periphery of the molecule, which correspond to the locations of the methyl groups and the oxygen atoms in the acetyl groups (Supplementary Fig. S3). This suggests that the lower-energy peak originates from the intrinsic π-orbitals of the conjugated DSB fragment, although the higher-energy one may result from the acetyl-derived resonance.

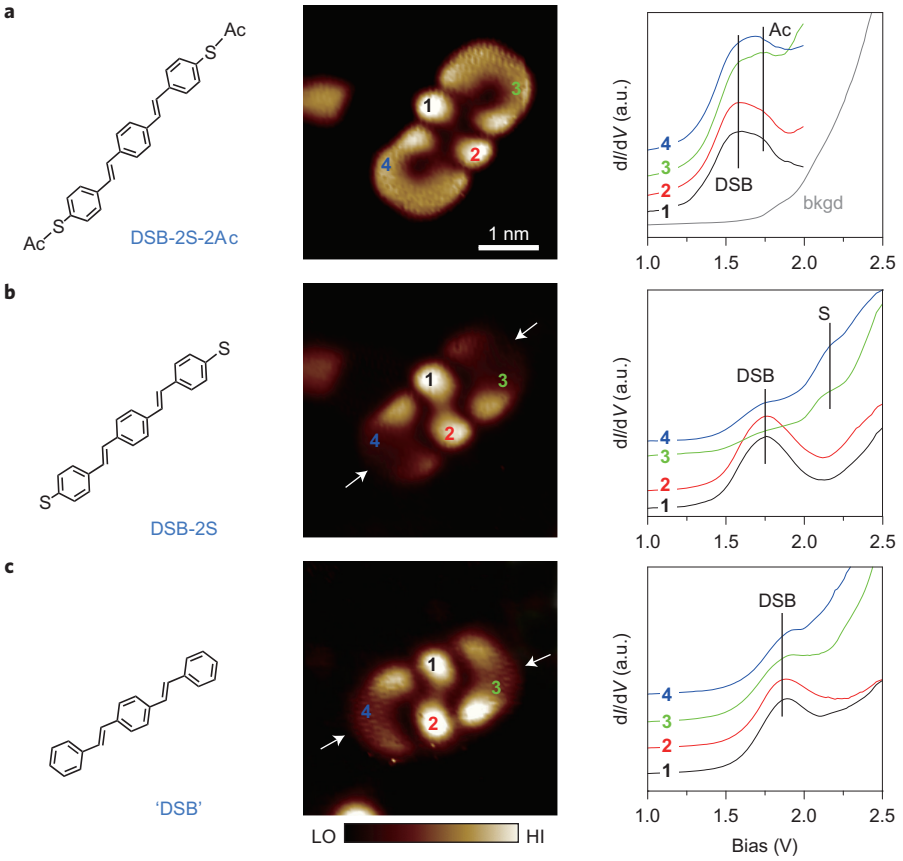

Figure 2 | Electronic structures of the molecules terminated with different functional groups. a–c, DSB-2S-2Ac (**a**), DSB-2S (**b**) and 'DSB' (**c**) molecules. Left, middle and right columns: scaled schematics (×1.8), dI/dV images and spatially resolved dI/dV spectra, respectively, of different molecules. Set point for acquiring the dI/dV images: $V = 1.6$ V, $I = 50$ pA. The dI/dV spectra (right column) were taken at four locations (1, 2, 3 and 4) on the molecules, as shown in the corresponding dI/dV images (middle column). The spectrum for bare NiAl(110) is denoted by 'bkgd' in the right column of (**a**). All the spectra were taken at the same set point ($V = 2.5$ V, $I = 0.1$ nA) and are offset for clarity. The energetic positions of the molecular resonances in the dI/dV spectra are highlighted by the vertical lines. The arrows in the middle column of (**b**) and (**c**) point to the changes in DOS from DSB-2S to 'DSB' (see the text for discussion). a.u. = arbitrary units.

In the acetyl-free molecule (DSB-2S), the DSB-derived state blue shifts to 1.75 V, and a new resonance state appears at 2.13 V (right column, Fig. 2b). The site-dependent dI/dV spectra indicate that the 2.13 V peak is localized at the ends of the molecule, which suggests that they originate from sulfur-derived states. The spatial imaging of the 1.75 V peak reveals that the π-orbitals of the molecule are suppressed dramatically at the ends where the acetyl groups were dissociated (arrows in the middle column of Fig. 2b). The absence of the π-electrons at the ends can be attributed to the strong σ-bonding between S 3p and C 2p, which tends to reduce the π-coupling within the conjugated molecule[30]. The attachment of the acetyl group to the sulfur atom can weaken the adjacent S–C σ-bond and thus facilitate the π-electrons spanning over the whole molecule.

Scissions of both sulfur atoms from DSB-2S result in an activated 'DSB', namely the DSB molecule with two terminal hydrogen atoms missing (left column, Fig. 2c). The site-dependent spectra exhibit the absence of the sulfur-derived resonance and a single peak at 1.90 V that corresponds to the π-resonance of 'DSB' (right column, Fig. 2c). Compared to DSB-2S, the π-orbital of 'DSB' partially recovers at the ends (arrows in the middle column of Fig. 2b and Fig. 2c), but is still less pronounced than that of the intact DSB (see Supplementary Fig. S4). This suggests that the 'DSB' molecule still has considerable σ-bonding with the substrate through the unsaturated C atoms.

The evolution of the π-resonance and the states derived from the functional groups are summarized quantitatively in Supplementary Fig. S5. The threshold biases for detaching the acetyl group (1.80 ± 0.20 V) and the sulfur atom (2.30 ± 0.15 V) correlate with the energies of Ac- and S-derived states, respectively. Therefore, the dissociations of the acetyl group and sulfur atom are associated with resonant electronic excitations, namely the transient attachment of the electrons to the Ac- and S-derived resonances[22–26]. The feasibility of submolecular control of bond-selective dissociation relies on the spatial localization and the energetic separation of the Ac- and S-derived states within the molecule.

Single-bond formation sequence. For the bond formation, we chose to investigate the Au–S interaction, which plays a decisive role in the fabrication of self-assembled monolayers[31] and studies of the charge transconductance across single molecules[17–21]. The images in Fig. 3a–f illustrate a typical Au–S bond-forming sequence. An intact DSB-2S-2Ac (**II**) was first activated by selectively dissociating the two acetyl groups to expose the sulfur anchoring atoms (arrows in Fig. 3a,b). Two single gold atoms (Au_L and Au_R in Fig. 3a) were then successively manipulated to the proximity of the exposed sulfur atoms (S_L and S_R in Fig. 3b) along pre-designed pathways (dotted lines in Fig. 3b,c). To explore the role of bonding geometry, these two gold atoms were attached to the molecule in different orientations. After bringing the reactants together, the gold atoms may not readily form strong chemical bonds with the sulfur atoms because of the higher energy barrier needed for bond formation than that for

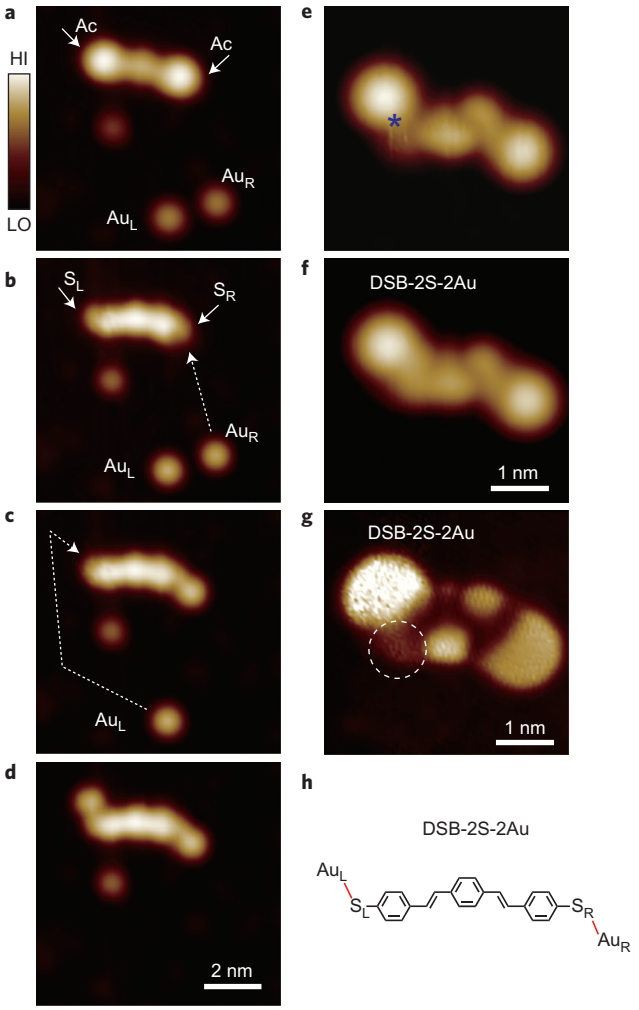

Figure 3 | Formation sequence of the DSB-2S-2Au complex. a–d, Manipulation sequence for attaching two gold atoms to a DSB-2S (**II**) molecule. The arrows in (**a**) indicate the acetyl groups and those in (**b**) the sulfur atoms. The dotted lines in (**b**) and (**c**) depict the trajectories along which the Au atoms were manipulated to the proximity of the molecule. The round protrusion below the molecule in (**a**) to (**d**) corresponds to an unknown impurity on the surface and can move around during the scanning. It does not interact with the adjacent molecule and the Au atoms. Set point for topographies: $V = 1.0$ V, $I = 50$ pA. The scale bar in **d** also relates to **a**–**c**. **e**,**f**, Zoom-in STM topographies before and after the formation of the Au_L–S_L covalent bond, respectively. The asterisk in (**e**) indicates the location at which 2.2 eV electrons were injected with the STM tip to form the Au_L–S_L covalent bond ('nanowelding'). The fuzzy feature below the asterisk in (**e**) arises from the instability of the molecule under the perturbation of the tip before the formation of the covalent bond. Set point for topographies: $V = 2.0$ V, $I = 50$ pA. The scale bar in **f** also relates to **e**. **g**, dI/dV image of the DSB-2S-2Au complex. Imaging conditions: $V = 1.6$ V, $I = 50$ pA. The dotted circle highlights the shared orbital structure in the Au_L–S_L covalent bond between the Au atom and the molecule. **h**, Scaled schematic model (×1.8) of the DSB-2S-2Au complex.

diffusion[7]. Such a transient state is shown in Fig. 3e, in which the Au_L–S_L bond can be perturbed easily by the STM tip (fuzzy lines in Fig. 3e). However, the reaction energy barrier can be overcome by injecting high-energy electrons (typically 2.2 eV) into the sulfur- and Au-derived resonances[22–26]. The resulting DSB-2S-2Au complex (Fig. 3f) shows local relaxation of the Au_L and S_L atoms. Recently, it was found that the thiolate actually bonds to Au adatoms instead of the extended Au surface[32,33]. Therefore, here single Au atoms are a good approximation to the Au electrodes that interact with the molecules in transconductance measurements.

Figure 3g shows the spatial map of the molecular resonance and the Au states in the DSB-2S-2Au complex. The dI/dV image of the acetyl-free molecule (DSB-2S) is shown in Supplementary Fig. S6 for comparison. The orbital of Au_L overlaps heavily with the π-system of the molecule and exhibits a distinct common orbital structure. Part of the electronic density of Au_L is modified and contributes to the DOS accumulation in the region between Au_L and the central part of the molecule (dashed circle in Fig. 3g), which is the most important characteristic of a covalent bond. In contrast, Au_R has less overlap with the molecule and shows a nodal structure between the Au_R orbital and the π-electrons, which suggests that the hybridization between Au_R and S_R is localized.

The dI/dV spectra taken at five key locations (denoted as 1, 2, 3, 4 and 5 in Fig. 4a) on the DSB-2S-2Au complex are presented in Fig. 4c–e. Owing to the localization of the states, the spectra obtained at 1, (2 and 3), and (4 and 5) mainly probe the DSB-, S- and Au-derived states, respectively. The spectra of DSB-2S and of the isolated Au atoms before the association are shown for comparison. The isolated Au atom adsorbed on NiAl(110) exhibits a single resonance peak at +2.09 V, which originates from the hybridization of Au 6s,p and NiAl states ('Free Au' in Fig. 4e)[28]. As the energy of the Au resonance can be affected by the adsorption site on the NiAl(110) surface, we always compare the Au atoms bonded to the DSB-2S and DSB-2S-Au with the isolated Au atom adsorbed at the same site (Supplementary Fig. S7). The 0.25 eV red shift of the Au_L state ('5' in Fig. 4e) and the 0.1 eV red shift of the S_L state ('3' in Fig. 4d) point to the formation of a strong covalent bond between Au_L and S_L that arises from the hybridization between the unpaired 3p electron of S_L and the sp electron of Au_L (ref. 34). In contrast, the Au_R state shifts to slightly higher energy by about 50 meV ('4' in Fig. 4e), which suggests that Au_R and S_R form a weak coordinate bond through the lone-pair electrons on S_R (ref. 35).

The mechanism of the bond formation is depicted schematically in Fig. 4b. The orientations of the unpaired electron and lone-pair electrons of the S atoms follow the symmetry of the DSB framework (mirror plane bisecting the internal aromatic ring). The formation of the covalent bond between the unpaired electrons on S_L and Au_L leads to the charge transfer from the Au_L to the molecule and the red shift of the Au_L state. The electron transfer into the lowest unoccupied DSB state of the molecule lowers its energy towards the Fermi level, which is consistent with the observed 0.15 eV red shift of the DSB state (Fig. 4c). In the coordinate bond, the lone-pair electrons on S_R are shared with Au_R, which results in the blue shift of the Au state on Au–S bond formation. In addition, the delocalization of the Au_L state and the localization of the Au_R state (as shown in Fig. 3g) provide further evidence for the formation of the covalent bond and the coordinate bond, respectively[35]. These observations demonstrate the possibility of selectively forming specific types of bonds by controlling the Au–S bonding geometry at the atomic scale.

Although the spatial distribution of the DSB-derived state remains almost unchanged in the middle part of the molecule on Au–S bond formation (Fig. 3g), the dI/dV spectrum is altered in terms of the energetic red shift (about 0.15 eV), the intensity reduction and the width broadening (Fig. 4c). These observations have important implications for electron transport through a single molecule that is in contact with metal leads[36]. The 0.15 eV energetic shift of the molecular resonance is prominent, as a 0.1 eV shift can change the conductance by nearly a factor of five (ref. 19). The reduced intensity and the broadened width of the molecular resonance reflect the shortened lifetime of the electron in the molecule, which may affect the extent of vibronic coupling within the molecule[36]. The changes in the electronic states of the molecule

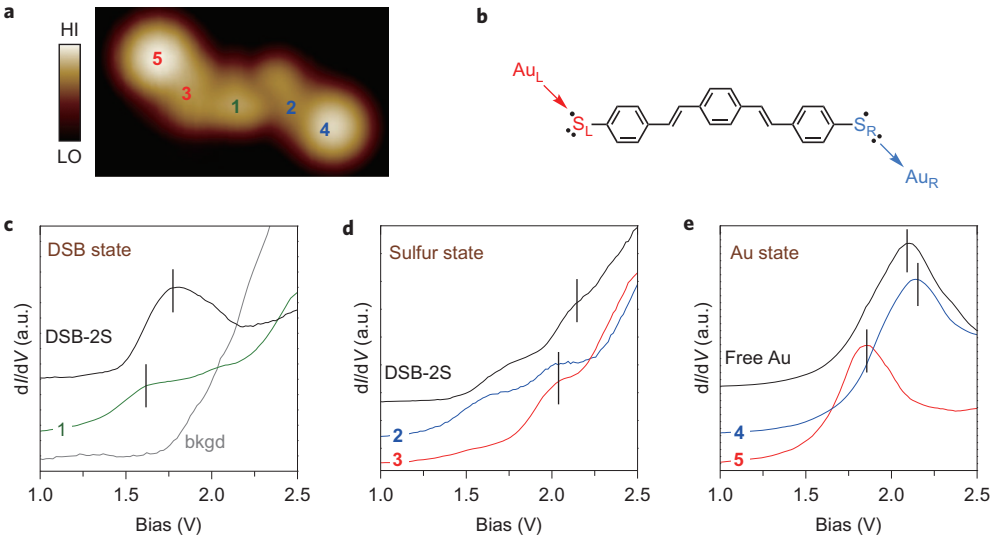

Figure 4 | Spatially resolved spectroscopy of the DSB-2S-2Au complex. a, Topographic image of the DSB-2S-2Au complex. Set point: $V = 1.6$ V, $I = 50$ pA. **b**, The schematic of the DSB-2S-2Au complex shows the covalent and coordinate Au–S bonds. Each S atom in DSB-2S has a lone pair of electrons and an unpaired electron, which are found to be oriented and maintain the symmetry of the DSB molecule. The arrows in the schematic denote the direction of the charge transfer between Au and S atoms. Set point: $V = 1.6$ V, $I = 50$ pA. **c**–**e**, dI/dV spectra taken at locations 1, 2, 3, 4 and 5 of the complex as indicated in (**a**) show states that originated from DSB, sulfur and Au, respectively. All the spectra were taken at the same set point ($V = 2.5$ V, $I = 0.1$ nA) and are offset for clarity. The energetic positions of the molecular resonances in the dI/dV spectra are highlighted by the vertical lines. Spectra denoted by 'DSB-2S' and 'Free Au' were taken on the acetyl-free molecule before the bond formation and on the isolated gold atom adsorbed at the same surface site as the Au_L and Au_R, respectively.

mean that the formation of the Au–S bond is expected to influence previously observed resonant electron transport, molecular charging and conformational change of the molecule.

For comparison, we performed the same experiments on the DSB-2S-2Ac (isomer **I**). The results of the bond formation for isomer **I** followed those for isomer **II**. The spectroscopy and imaging of a DSB-2S-2Au complex (isomer **I**), in which both Au atoms formed covalent bonds with the S atoms, are shown in Supplementary Fig. S8.

Conclusions

We systematically investigated single-bond dissociation and formation in a functionalized π-conjugated molecule. The selective dissociation was realized by locally injecting the energy-tunable electrons into the corresponding resonant molecular states. The influence of the different functional groups on the energetic positions and spatial distributions of the molecular resonance was determined by studying the evolution of the electronic structure of single molecules. In addition to bond-selected dissociation, we further investigated the Au–S interaction by manipulating single gold atoms to form covalent and coordinate bonds between the Au atoms and the S-activated molecule. The modifications of the molecular resonance on the Au–S bond formation, the directionality of the Au–S bond and the extent of the Au–S coupling were revealed and may clarify the long-standing discrepancy of the electron transport in thiol-based molecular junctions. This work also opens up the possibility of measuring electron transport, controlled with atomic precision, through a single thiol-based molecule in an electrode–molecule contact geometry.

Methods

The experiments were carried out with a home-built, ultra-high vacuum, low-temperature STM operated at 12 K (ref. 37), with the base pressure better than 2.0×10^{-11} torr. The NiAl(110) single crystal was cleaned by repeated cycles of Ne^+ sputtering and annealing. Then, individual DSB-2S-2Ac molecules[38] and gold atoms were evaporated thermally *in situ* onto the surface at 12 K. All the STM measurements were performed at 12 K with silver tips, which were cleaned by three cycles of annealing and sputtering before the experiments, and further by controlled field-emission and tip-crash procedures on the surface. Bias voltage refers to the sample voltage with respect to the tip. All the STM topographic images were obtained in the constant current mode. For scanning tunnelling spectroscopy measurements, a modulation frequency of 243 Hz and amplitude of 10 mV were adopted in the lock-in detection of the differential conductance spectra and images. The manipulation of the Au atoms was realized in the so-called 'pulling mode'. A typical condition for the manipulation in our experiment was with a sample bias of 7 mV and a tunnelling current of 60 nA. To achieve bond-selective dissociation, the STM tip was held at a fixed position over a selected part of the molecule (indicated by the asterisks in Fig. 1f), followed by raising the tunnelling current to 1 nA. Then the sample bias was gradually ramped up from the imaging conditions (typically 1 V) with the feedback on. To avoid any further additional changes in the molecule, the bias was decreased quickly back to the imaging condition on detection of a sudden jump in the tip height associated with the bond dissociation (Fig. 1e).

Received 8 May 2012; accepted 26 September 2012; published online 11 November 2012

References

1. Jortner, J., Levine, R. D. & Pullman, B. *Mode Selective Chemistry* (Kluwer Academic, 1991).
2. Crim, F. F. Bond-selected chemistry: vibrational state control of photodissociation and bimolecular reaction. *J. Phys. Chem.* **100,** 12725–12734 (1996).
3. Ho, W. Inducing and viewing bond selected chemistry with tunneling electrons. *Acc. Chem. Res.* **31,** 567–573 (1998).
4. Hla, S. W. & Rieder, K. H. STM control of chemical reactions: single-molecule synthesis. *Annu. Rev. Phys. Chem.* **54,** 307–330 (2003).
5. Stipe, B. C. *et al.* Single molecule dissociation by tunneling electrons. *Phys. Rev. Lett.* **78,** 4410–4413 (1997).
6. Lee, H. J. & Ho, W. Single-bond formation and characterization with a scanning tunneling microscope. *Science* **286,** 1719–1722 (1999).
7. Hla, S. W., Bartels, L., Meyer, G. & Rieder, K. H. Inducing all steps of a chemical reaction with the scanning tunneling microscope tip: towards single molecule engineering. *Phys. Rev. Lett.* **85,** 2777–2780 (2000).
8. Lauhon, L. J. & Ho, W. Control and characterization of a multistep unimolecular reaction. *Phys. Rev. Lett.* **84,** 1527–1530 (2000).
9. Pascual, J. I., Lorente, N., Song, Z., Conrad, H. & Rust, H-P. Selectivity in vibrationally mediated single-molecule chemistry. *Nature* **423,** 525–528 (2003).
10. Sloan, P. A. & Palmer, R. E. Two-electron dissociation of single molecules by atomic manipulation at room temperature. *Nature* **434,** 367–371 (2005).
11. Repp, J., Meyer, G., Paavilainen, S., Olsson, F. E. & Persson, M. Imaging bond formation between a gold atom and pentacene on an insulating surface. *Science* **312,** 1196–1199 (2006).

12. Gawronski, H., Carrasco, J., Michaelides, A. & Morgenstern, K. Manipulation and control of hydrogen bond dynamics in absorbed ice nanoclusters. *Phys. Rev. Lett.* **101,** 136102 (2008).
13. Sakulsermsuk, S., Sloan, P. A. & Palmer, R. E. A new mechanism of atomic manipulation: bond-selective molecular dissociation via thermally activated electron attachment. *ACS Nano* **4,** 7344–7348 (2010).
14. Shin, H. J. *et al.* State-selective dissociation of a single water molecule on an ultrathin MgO film. *Nature Mater.* **9,** 442–447 (2010).
15. Kumagai, T. *et al.* H-atom relay reactions in real space. *Nature Mater.* **11,** 167–172 (2012).
16. Pauling, L. *The Nature of the Chemical Bond* (Cornell University Press, 1960).
17. Reed, M. A., Zhou, C., Muller, C. J., Burgin, T. P. & Tour, J. M. Conductance of a molecular junction. *Science* **278,** 252–254 (1997).
18. Li, X. *et al.* Conductance of single alkanedithiols: conduction mechanism and effect of molecule–electrode contacts. *J. Am. Chem. Soc.* **128,** 2135–2141 (2006).
19. Yaliraki, S. N., Kemp, M. & Ratner, M. A. Conductance of molecular wires: influence of molecule–electrode binding. *J. Am. Chem. Soc.* **121,** 3428–3434 (1999).
20. Bratkovsky, A. M. & Kornilovitch, P. E. Effects of gating and contact geometry on current through conjugated molecules covalently bonded to electrodes. *Phys. Rev. B* **67,** 115307 (2003).
21. Chen, F., Hihath, J., Huang, Z., Li, X. & Tao, N. J. Measurement of single-molecule conductance. *Annu. Rev. Phys. Chem.* **58,** 535–564 (2007).
22. Antoniewicz, P. R. Model for electron- and photon-stimulated desorption. *Phys. Rev. B* **21,** 3811–3815 (1980)
23. Bartels, L. *et al.* Dynamics of electron-induced manipulation of individual CO molecules on Cu(111). *Phys. Rev. Lett.* **80,** 2004–2007 (1998).
24. Qiu, X. H., Nazin, G. V. & Ho, W. Mechanisms of reversible conformational transitions in a single molecule. *Phys. Rev. Lett.* **93,** 196806 (2004).
25. Iancu, V. & Hla, S. W. Realization of a four-step molecular switch in scanning tunneling microscope manipulation of single chlorophyll-a molecules. *Proc. Natl Acad. Sci. USA* **103,** 13718–13721 (2006).
26. Lastapis, M. *et al.* Picometer-scale electronic control of molecular dynamics inside a single molecule. *Science* **308,** 1000–1003 (2005).
27. Seferos, D. S., Trammell, S. A., Bazan, G. C. & Kushmerick, J. G. Probing π-coupling in molecular junctions. *Proc. Natl Acad. Sci. USA* **102,** 8821–8825 (2005).
28. Nilius, N., Wallis, T. M., Persson, M. & Ho, W. Distance dependence of the interaction between single atoms: gold dimers on NiAl(110). *Phys. Rev. Lett.* **90,** 196103 (2003).
29. Lauhon, L. J. & Ho, W. Single molecule chemistry and vibrational spectroscopy: pyridine and benzene on Cu(001). *J. Phys. Chem. A* **104,** 2463–2467 (2000).
30. Schwingenschlögl, U. & Schuster, C. Electronic structure of the Au/benzene-1,4-dithiol/Au transport interface: effects of chemical bonding. *Chem. Phys. Lett.* **435,** 100–103 (2007).
31. Love, J. C., Estroff, L. A., Kriebel, J. K., Nuzzo, R. G. & Whitesides, G. M. Self-assembled monolayers of thiolates on metals as a form of nanotechnology. *Chem. Rev.* **105,** 1103–1169 (2005).
32. Yu, M. *et al.* True nature of an archetypal self-assembly system: mobile Au–thiolate species on Au(111). *Phys. Rev. Lett.* **97,** 166102 (2006).
33. Cossaro, A. *et al.* X-ray diffraction and computation yield the structure of alkanethiols on gold(111). *Science* **321,** 943–946 (2008).
34. Bratkovsky, A. M. & Kornilovitch, P. E. Effects of gating and contact geometry on current through conjugated molecules covalently bonded to electrodes. *Phys. Rev. B* **67,** 115307 (2003).
35. Ning, Z. Y., Ji, W. & Guo, H. Role of contact formation process in transport properties of molecular junctions: conductance of Au/BDT/Au molecular wires. *Mesoscale Nanoscale Phys.* http://arxiv.org/abs/0907.4674 (2010).
36. Galperin, M., Ratner, M. A., Nitzan, A. & Trosi, A. Nuclear coupling and polarization in molecular transport. *Science* **319,** 1056–1060 (2008).
37. Stipe, B. C., Rezaci, M. A. & Ho, W. A variable-temperature scanning tunneling microscope capable of single-molecule vibrational spectroscopy. *Rev. Sci. Instrum.* **70,** 137–143 (1999).
38. Seferos, D. S., Banach, D. A., Alcantar, N. A., Israelachvili, J. N. & Bazan, G. C. α,ω-Bis(thioacetyl)oligophenylenevinylene chromophores from thioanisol precursors. *J. Org. Chem.* **69,** 1110–1119 (2004).

Acknowledgements

The authors thank W. Ji and C. Chen for helpful discussions. This work was supported by the National Science Foundation Center for Chemical Innovation on Chemistry at the Space–Time Limit (CaSTL) under Grant CHE-0802913, the National Basic Research 973 Programs of China under Grant 2012CB921303, and the Chemical Science, Geo- and Bioscience Division, Office of Science, US Department of Energy, under Grant DE-FG02-06ER15826. In addition, Y.J. acknowledges support from the National Science Foundation of China under Grants 11104004 and 91021007, and the Research Fund for the Doctoral Program of Higher Education of China under Grant 20110001120126.

Author contributions

W.H. designed and supervised the project. Y.J. and Q.H. performed the measurements and analysed the data, and contributed equally to this work. L.F. and G.C.B. synthesized the DSB-2S-2Ac molecules. Y.J. and W.H. co-wrote the manuscript. The manuscript reflects the contributions of all the authors.

Additional information

Supplementary information is available in the online version of the paper. Reprints and permission information is available online at http://www.nature.com/reprints. Correspondence and requests for materials should be addressed to W.H.

Competing financial interests

The authors declare no competing financial interests.